AGU100 ADVANCING EARTH AND SPACE SCIENCE

Geophysical Research Letters

RESEARCH LETTER
10.1029/2018GL078242

Key Points:
- Anomalous energy budget of ocean mixed layer associated with northeast Pacific marine heatwave off Baja California is quantified
- Record deficit in low clouds and increase in downwelling radiation implicate positive cloud feedback as key to the warming off Baja
- Results demonstrate importance of low clouds in regional climate variability

Supporting Information:
- Supporting Information S1

Correspondence to:
T. A. Myers,
tamyers@ucla.edu

Citation:
Myers, T. A., Mechoso, C. R., Cesana, G. V., DeFlorio, M. J., & Waliser, D. E. (2018). Cloud feedback key to marine heatwave off Baja California. *Geophysical Research Letters*, *45*, 4345–4352. https://doi.org/10.1029/2018GL078242

Received 30 DEC 2017
Accepted 19 APR 2018
Accepted article online 30 APR 2018
Published online 9 MAY 2018

Cloud Feedback Key to Marine Heatwave off Baja California

Timothy A. Myers[1], Carlos R. Mechoso[1], Gregory V. Cesana[2,3], Michael J. DeFlorio[4], and Duane E. Waliser[4]

[1]Department of Atmospheric and Oceanic Sciences, University of California, Los Angeles, CA, USA, [2]Department of Applied Physics and Mathematics, Columbia University, New York, NY, USA, [3]NASA Goddard Institute for Space Studies, New York, NY, USA, [4]Jet Propulsion Laboratory, California Institute of Technology, Pasadena, CA, USA

Abstract Between 2013 and 2015, the northeast Pacific Ocean experienced the warmest surface temperature anomalies in the modern observational record. This "marine heatwave" marked a shift of Pacific decadal variability to its warm phase and was linked to significant impacts on marine species as well as exceptionally arid conditions in western North America. Here we show that the subtropical signature of this warming, off Baja California, was associated with a record deficit in the spatial coverage of co-located marine boundary layer clouds. This deficit coincided with a large increase in downwelling solar radiation that dominated the anomalous energy budget of the upper ocean, resulting in record-breaking warm sea surface temperature anomalies. Our observation-based analysis suggests that a positive cloud-surface temperature feedback was key to the extreme intensity of the heatwave. The results demonstrate the extent to which boundary layer clouds can contribute to regional variations in climate.

Plain Language Summary The northeast Pacific Ocean experienced a "marine heatwave" between 2013 and 2015. This was characterized by the highest surface temperatures ever recorded in a vast swath of the ocean from near the Gulf of Alaska to off the coast of Baja California. The unprecedented warming event was linked to significant impacts on marine life and a severe drought in western North America. We analyze satellite data to show that the heatwave was associated with a record decrease in the typically high cloudiness over an area of the Pacific off Baja California that is roughly half the size of the contiguous United States. Such a deficit in cloud cover coincided with a large increase in the amount of sunlight absorbed by the ocean surface, resulting in extremely warm temperatures. Our findings suggest that a reinforcing interaction (or positive feedback) between clouds and ocean surface temperature can strongly contribute to significant and difficult-to-predict changes in marine climate.

1. Introduction

In late 2013, an unusually warm water mass or "Blob" appeared in the midlatitude northeast (NE) Pacific near the Gulf of Alaska, reaching surface temperatures higher than any observed since at least the early 1980s (Amaya et al., 2016; Bond et al., 2015). This warming has been attributed to reduced ocean-to-atmosphere heat flux associated with weaker surface winds and an anomalous high-pressure ridge over the far north Pacific, which also contributed to a severe drought in western North America (Bond et al., 2015; Seager et al., 2015; Swain et al., 2014). In the subsequent two years, further record-breaking warming occurred throughout the NE Pacific, from the midlatitudes to the subtropics (Amaya et al., 2016; Gentemann et al., 2017; Zaba & Rudnick, 2016). This "marine heatwave" was coincident with a transition of the Pacific Decadal Oscillation (PDO) to its warm phase (Su et al., 2017). Elevated surface temperatures were associated with a sharp phytoplankton reduction and toxic algal bloom along the western North American coast, negatively impacting fisheries (Cavole et al., 2016). It has been argued that tropical-extratropical teleconnections involving the weak boreal fall 2014 El Niño led to the widespread NE Pacific warming patterns in 2014 and 2015 that followed the emergence of the midlatitude NE Pacific Blob in 2013 (Di Lorenzo & Mantua, 2016). It has also been suggested that dynamics involving the very strong El Niño that peaked in magnitude in late 2015 contributed to the ocean warming signal of the marine heatwave along the western Baja California coast (Robinson, 2016) and, more broadly, to the signal along the western North American coast (Jacox et al., 2018). However, no study has quantified the local forcing mechanisms of the robust signal of the marine heatwave in the subtropical region of the NE Pacific off Baja California, from an energy budget perspective. Here we examine these local contributions through an observational analysis of the energy budget of the upper ocean.

The climate of the subtropical NE Pacific is characterized by cool sea surface temperature (SST) compared to the zonal mean accompanied by extensive and persistent stratiform clouds occurring within the planetary boundary layer. These clouds reflect up to around 100 W/m^2 (>20%) of incoming solar radiation back to space (Hartmann et al., 1992) and are tightly coupled to fluctuations in underlying SST. Relatively warmer SST suppresses overlying cloudiness by altering vertical gradients of temperature and moisture (Bretherton et al., 2013; Klein et al., 2017; Klein & Hartmann, 1993; Rieck et al., 2012; van der Dussen et al., 2015). In turn, suppressed cloudiness allows more solar radiation to reach the underlying ocean surface, further increasing SST. Alternatively, relatively cooler SST promotes cloudiness, further decreasing SST. Model-based evidence suggests that this positive cloud-SST feedback amplifies anomalies, regardless of their sign, from the climatological mean SST (Bellomo et al., 2014, 2015, 2016; Brown et al., 2016; Burgman et al., 2017; Myers et al., 2017, 2018). To what extent did this feedback contribute to the marine heatwave in the stratiform cloud region off Baja California? We address this question by using observation-based data to quantify the contributions of surface radiative and turbulent heat fluxes and oceanic processes to the energy budget of the ocean mixed layer in the nearly two-year period of anomalously warm SST in the region that peaked roughly in September 2015.

2. Data and Methods

We express the anomalous mixed layer energy budget at each grid box and month as

$$\left(\rho c_p h \partial T/\partial t\right)' = F'_{\mathrm{rad}} + F'_{\mathrm{turb}} - \left(\rho c_p h(\boldsymbol{V}\cdot\nabla T)\right)' + \mathrm{RES}'. \quad (1)$$

Here primes denote anomalies from climatological monthly means (i.e., deviations from the seasonal cycle), ρ = 1,025 kg/m^3 is the density of seawater, c_p = 3994 J · kg^{-1} · K^{-1} is the specific heat of seawater at constant pressure, h is depth of the mixed layer, T is vertically averaged temperature in the mixed layer, F'_{rad} is anomalous net (downwelling minus upwelling) surface radiative flux, F'_{turb} is anomalous surface turbulent (sensible plus latent) heat flux, $\boldsymbol{V}$ is vertically averaged horizontal velocity in the mixed layer, and RES$'$ is a residual flux computed to close the budget that is inferred to be due to vertical mixing at the base of the mixed layer. Equation (1) can be written as

$$\left(\rho c_p h \partial T/\partial t\right)' = F'_{\mathrm{rad}} + F'_{\mathrm{turb}} + F'_{\mathrm{ocean}} \quad (2)$$

where $F'_{\mathrm{ocean}} = -\left(\rho c_p h(\boldsymbol{V}\cdot\nabla T)\right)' + \mathrm{RES}'$ is the anomalous total oceanic heat flux into the mixed layer due to horizontal advection and vertical mixing.

We obtain observation-based estimates of h, temperature, and horizontal velocity from the National Centers for Environmental Prediction Global Ocean Data Assimilation System (GODAS), which is constructed from a numerical ocean model with assimilation of ocean profile observations and given on a 1/3° latitude × 1° longitude grid (Behringer, 2007; Behringer & Xue, 2004). h is a product of a K-profile parameterization mixing scheme (Large et al., 1994). T and $\boldsymbol{V}$ are computed as the vertically averaged temperature and horizontal velocity spanning all model levels (given at 10-meter resolution) centered at or above h. The temperature tendency $\partial T/\partial t$ is approximated at each month t as T for the subsequent month subtracted by T for the previous month, divided by two months. T and h were bilinearly interpolated to a 1° × 1° grid in order for $\rho c_p h \partial T/\partial t$ to match the resolution of the other data sets. $\boldsymbol{V}\cdot\nabla T$ is approximated using centered finite differencing in spherical coordinates using the native GODAS grid, which was then bilinearly interpolated to a 1° × 1° grid. Practically identical results are obtained if we substitute T with SST from the National Oceanic and Atmospheric Administration (NOAA) Optimum Interpolation (OI) SST data set V2 (Reynolds et al., 2002), which is given on a 1° × 1° grid.

F_{rad} is provided by the Clouds and the Earth's Radiant Energy System (CERES) Energy Balanced and Filled data set version 2.8, given on a 1° × 1° grid (Kato & Loeb, 2013). This product is based on a radiative transfer model that estimates surface radiative fluxes using cloud, aerosol, temperature, and humidity information from satellite retrievals and an atmospheric reanalysis. Importantly, the estimated surface fluxes are physically consistent with satellite measurements of radiation at the top of the atmosphere. Two estimates of F_{turb} are taken from the Objectively Analyzed Air-sea Fluxes (OAFlux) Project (Yu, Jin, & Weller, 2008), given on a 1° × 1° grid, and the European Centre for Medium-Range Weather Forecasts Interim Re-Analysis (ERA-Interim; Dee et al., 2011), which was bilinearly interpolated to a 1° × 1° grid. OAFlux provides estimates of surface sensible and

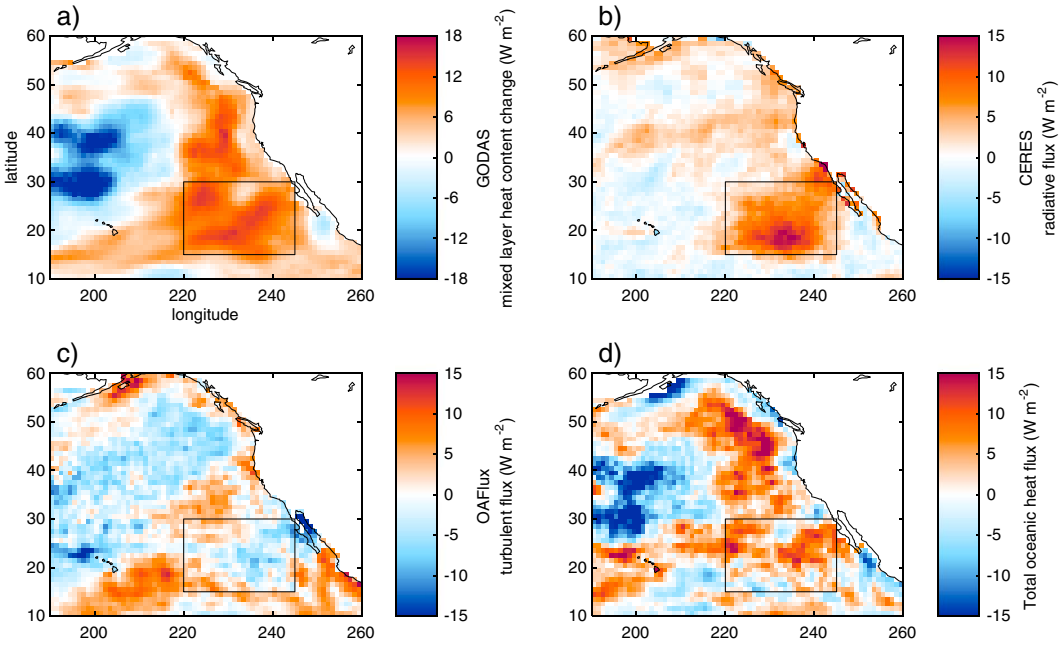

Figure 1. Components of anomalous energy budget of ocean mixed layer during January 2014 to September 2015, including temporally averaged (a) $(\rho c_p h \partial T/\partial t)'$ from GODAS, (b) F'_{rad} from CERES, (c) F'_{turb} from OAFlux, and (d) F'_{ocean} obtained as a residual in equation (2). Anomalies are relative to 2001–2015 climatological monthly means. Positive values indicate energy gained by the ocean. The maximum warming region is outlined in black.

latent heat fluxes using bulk flux parameterizations and objective analysis of surface meteorological information from satellite retrievals and three different atmospheric reanalyses. ERA-Interim predicts surface sensible and latent heat fluxes using an atmospheric forecast model initialized by observations.

3. Mixed Layer Energy Budget off Baja California During the Marine Heatwave

Figure 1a shows the month-to-month change in anomalous heat content of the ocean mixed layer, $(\rho c_p h \partial T/\partial t)'$, averaged between January 2014 and September 2015. This quantity represents the energy gained by the mixed layer during this period, revealing a core of maximum heating in the region off Baja California outlined in black (15°N–30°N, 220°E–245°E). This accumulation of energy spans the approximate onset and peak of anomalously warm SST that occurred in this region, where temperatures reached values higher than any observed since 1951 (Figures 2a and S1 and Text S1; September 2015 was the month just before the peak SST; Huang et al., 2014). Contemporaneously, the PDO shifted to its warm phase (Figure S1).

The average surface radiative flux monthly anomalies, F'_{rad}, from CERES are strongly positive over the core of maximum warming (Figure 1b), with a spatial mean of 6.7 ± 1.8 W/m^2 (95% sampling uncertainty; Text S2) over the outlined region. This value was the strongest 21-month running mean anomaly centered outside of 2014 and 2015 in the CERES record (Figure 2b). Observed average turbulent heat flux monthly anomalies, F'_{turb}, from OAFlux are small and mostly negative over the warming core, with a spatial mean of −0.6 ± 2.2 W/m^2 that is not significantly different from zero (Figure 1c). The average total oceanic heat flux monthly anomalies, F'_{ocean}, are mostly positive over the region, with a spatial mean of 3.8 ± 3.3 W/m^2 (Figure 1d). About half of the total oceanic flux appears to have been due to anomalously positive yet statistically insignificant horizontal advection, $-(\rho c_p h(\boldsymbol{V}\cdot\nabla T))'$ (Table 1, bottom row, and Figure S2). The other half is attributable to anomalously positive yet statistically insignificant residual oceanic flux, RES$'$, presumably due to weaker-than-average vertical mixing at the base of the mixed layer (Table 1, bottom row, and Figure S2). Spatially averaged values of F'_{turb}, F'_{ocean}, and RES$'$ computed using ERA-Interim turbulent flux data instead are similar to those obtained using OAFlux (Table 1, bottom row).

These results show that anomalously positive radiative flux was the dominant component of the energy budget of the ocean mixed layer during this period of warming off Baja California, implicating the

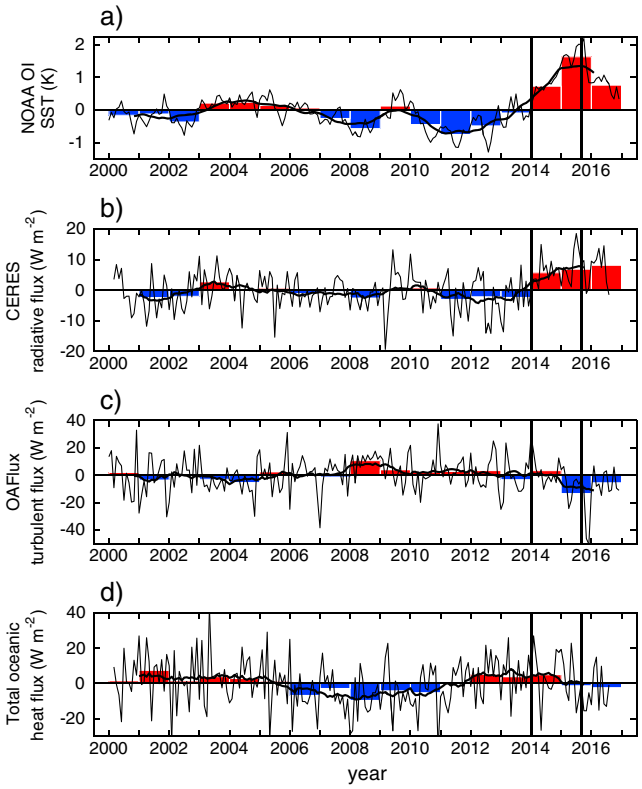

Figure 2. Time series of anomalies relative to 2001–2015 climatological monthly means of (a) NOAA OI SST, (b) F'_{rad} from CERES, (c) F'_{turb} from OAFlux, and (d) F'_{ocean} computed as a residual in equation (2) averaged over the subtropical NE Pacific (15°N–30°N, 220°E–245°E, outlined in black in Figure 1). In each panel, the thin black line, bars, and thick black line represent monthly mean, annual mean, and 21-month running mean anomalies, respectively. Running means are computed for a given month by averaging the monthly means 10 months before to 10 months after that month. The thick vertical lines demarcate the approximate onset and peak of the record-breaking warm SST anomalies.

atmosphere as a driver of the ocean heating. Radiative flux anomalies were also large and positive in each of two shorter nonoverlapping intervals collectively spanning January 2014 to September 2015, separated according to when turbulent heat flux anomalies changed from positive to strongly negative in early boreal spring 2015 and when the total oceanic heat flux ceased to be positive (Table 1, top two rows, and Figures 2c and 2d and S3 and S4). In the first interval, reduced heat loss from the ocean to the atmosphere and suppressed vertical mixing in the upper ocean were likely induced by weaker trade winds associated with an expansive anomalous cyclone in the NE Pacific (Figure S5). Independent observational analyses also suggest that suppressed vertical mixing and upwelling associated with weak winds contributed to warm SST anomalies along the Southern California and western Baja California coastlines in 2014 and 2015 (Robinson, 2016; Zaba & Rudnick, 2016). The anomalous cyclone and associated turbulent and oceanic fluxes were likely driven in part by the boreal fall 2014 El Niño (Amaya et al., 2016; Di Lorenzo & Mantua, 2016). Model simulations also suggest a link between El Niño and subtropical NE Pacific SST anomalies via alteration of wind-driven surface fluxes (Yu, Liu, & Mechoso, 2000). Relaxed-trades-driven warming was then followed by enhanced sensible and latent heat loss caused by very warm SST in the second interval (Figures 2a and 2c and S4), marking the emergence of the negative turbulent heat flux feedback (Park et al., 2005). Even during this latter period of turbulent heat flux damping, very warm SST persisted due to anomalously positive radiative flux.

4. Role of Low Clouds

Next we identify which atmospheric process caused the increase in absorbed surface radiation responsible for much of the anomalous ocean heating. Figure 3a reveals that total cloud fraction retrieved by the Moderate Resolution Imaging Spectroradiometer (MODIS) onboard the TERRA satellite (Minnis et al., 2011; Text S1) between January 2014 and September 2015 over the subtropical NE Pacific was much smaller than average. Moreover, the maximum negative anomalies were co-located with those of radiative flux. The negative anomalies resulted from reduced coverage of boundary layer clouds, as captured by vertically resolved cloud fraction from the Cloud–Aerosol Lidar and Infrared Pathfinder Satellite Observations (CALIPSO; Chepfer et al., 2010; Cesana et al., 2016), illustrated in Figure 3b. The CALIPSO observations show a decrease of cloud amount below 2 km within the warming region. The negative low-level cloud fraction anomalies had their strongest 21-month running mean value since 2001 and possibly since 1984 (Figures 3c and S6; Garay et al.,

Table 1
Components of Anomalous Energy Budget of Ocean Mixed Layer Spatially Averaged Over the Subtropical NE Pacific (15°N–30°N, 220°E–245°E, Outlined in Black in Figure 1) and Temporally Averaged Over Different Time Periods Described in the Text

	F'_{rad}	F'_{turb}		F'_{ocean}		$-(\rho c_p h(\mathbf{V}\cdot\nabla T))'$	RES′	
	CERES	OAFlux	ERA	OAFlux	ERA	GODAS	OAFlux	ERA
January 2014 to February 2015	***5.5 ± 1.6***	***3.6 ± 2.6***	***5.8 ± 3.8***	***6.4 ± 4.2***	4.2 ± 5.3	0.8 ± 2.8	***5.5 ± 4.5***	3.3 ± 5.6
March 2015 to September 2015	***9.1 ± 3.7***	***−9.2 ± 2.9***	***−14.3 ± 6.1***	−1.4 ± 5.2	3.7 ± 7.8	3.7 ± 7.4	−5.2 ± 6.1	0 ± 8.7
January 2014 to September 2015	***6.7 ± 1.8***	−0.6 ± 2.2	−0.9 ± 3.8	***3.8 ± 3.3***	4 ± 4.1	1.8 ± 3.3	1.9 ± 3.9	2.2 ± 5

Note. Also shown is/are the data set /s used to compute each term. Units are W/m^2. The error bars span 95% confidence intervals, and boldface and italicized text indicates statistical significance at the 95% level.

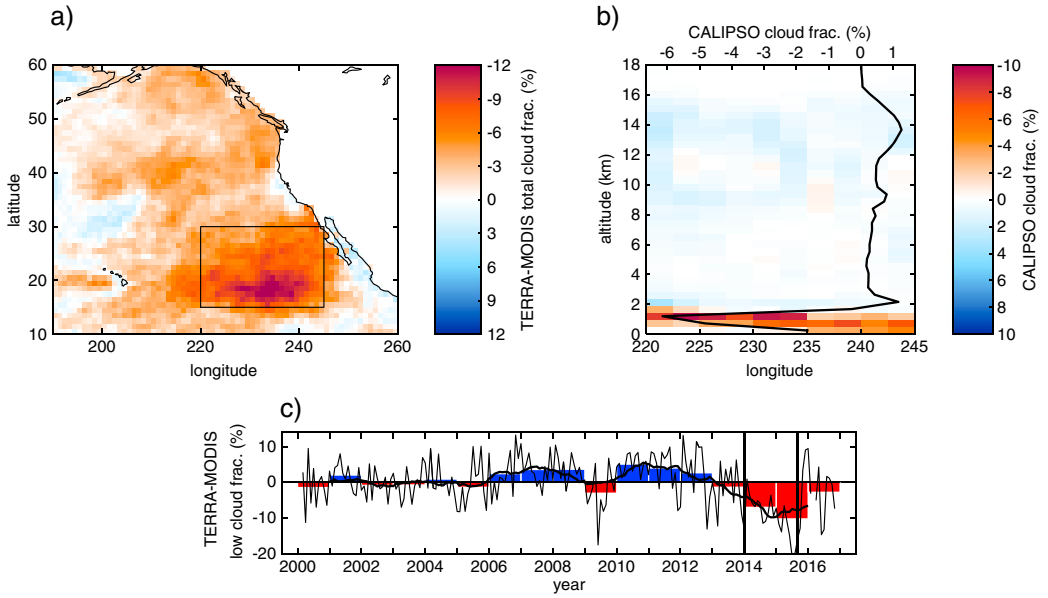

Figure 3. (a) Total cloud fraction anomalies relative to 2001–2015 climatological monthly means from TERRA-MODIS averaged from January 2014 to September 2015, (b) spatial and meridional mean cloud fraction anomalies relative to 2007–2016 climatological monthly means as a function of altitude from CALIPSO averaged over the same period, and (c) time series of subtropical NE Pacific low-level cloud fraction anomalies relative to 2001–2015 climatological monthly means from TERRA-MODIS. The averages in (b) and (c) are computed within the region outlined in black in (a). The lines and bars in (c) are as in Figure 2. Note that the red shading and bars indicate negative cloud fraction anomalies, while the blue indicates positive anomalies.

2008; Norris & Evan, 2015; Rossow & Schiffer, 1999). In a similar cloud regime in the Atlantic, it has been estimated that a one percent reduction in cloud fraction generates an additional 0.77 W/m^2 of net radiation absorbed by the ocean surface (Bellomo et al., 2016). Using this value and the average of TERRA-MODIS, AQUA-MODIS, and CALIPSO negative low-level cloud fraction anomalies of ~9 ± 1.3% (long-term annual mean cloud fraction is 57%; Text S1 and S2), we estimate that an additional 6.9 ± 1 W/m^2 of radiation was absorbed by the subtropical NE Pacific Ocean between January 2014 and September 2015. Since this is nearly identical to the anomalous surface radiative flux from CERES noted above and to the average anomalous surface net cloud radiative effect (CRE) during this period (7 ± 1.8 W/m^2; Figure S7), we conclude that the increase in downwelling radiation was caused by a reduction in stratiform cloud coverage.

Thus, once warm SST anomalies in the subtropical NE Pacific were established in early 2014, a positive feedback between SST and stratiform cloudiness was a critical amplifier of the warm anomalies that kept increasing to unprecedented levels until late 2015, despite the emergence of strong turbulent heat flux damping. This amplifying process therefore likely contributed to the transition of the PDO to its warm phase, which corroborates model evidence suggesting that a positive cloud feedback drove a large portion of the PDO's shift to its cool phase in the late 1990s (Burgman et al., 2017). The feedback moreover may have contributed indirectly to the very strong 2015/2016 El Niño if the subtropical SST anomalies were communicated to the equatorial tropics through meridional mode dynamics (Feng et al., 2014; Paek et al., 2017; Tseng et al., 2017). Finally, the importance of this reinforcing cloud-SST interaction off Baja California was not restricted to the marine heatwave, as suggested by the positive correlation between regional anomalies of surface radiative flux (Figure 2b) and SST (Figure 2a; r = 0.6 and r = 0.9 for unfiltered and 21-month running mean monthly anomalies, respectively).

5. Energy Budget of the Blob

Given the evidence for the importance of cloud feedback in the Baja California region of the NE Pacific marine heatwave, such a process might also have played a role in locally amplifying the warm SST Blob anomaly in the midlatitude NE Pacific that emerged in 2013, especially since stratiform clouds are abundant during boreal summer in this region (Klein & Hartmann, 1993). We address this possibility with the same observations and techniques used so far in the paper. Figure 4 shows the components of the anomalous mixed

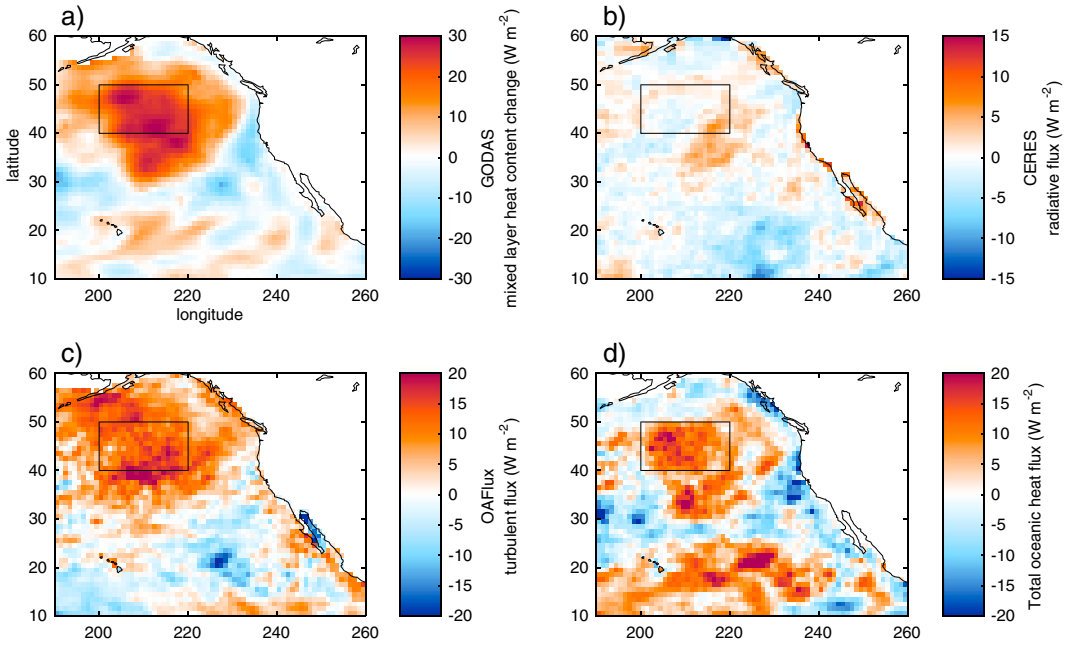

Figure 4. As in Figure 1 but for January 2013 to December 2013.

layer energy budget averaged between January and December 2013, when warm SST anomalies in the midlatitude NE Pacific (40°N–50°N, 200°E–220°E) sharply increased to their peak (Figure S8; December 2013 was the month just before the peak SST). Even though low-level cloud fraction was reduced slightly over the core of maximum heating in the midlatitude NE Pacific during this period and much more so afterward when warm SST anomalies persisted (Figures 4a and S9), radiative flux anomalies were negligible, with spatially averaged annual means of 0.4 ± 1.7 W/m^2 in 2013 and 0 ± 1 W/m^2 in 2014 (Figures 4b and S8). This phenomenon can be explained by the substantial offset between positive anomalies of surface shortwave CRE and negative anomalies of longwave CRE, having spatial mean values over the midlatitude NE Pacific of 2.5 ± 1.7 and −3.2 ± 0.9 W/m^2 in 2013 and 3.5 ± 1.5 and −3.4 ± 1 W/m^2 in 2014 (Figure S10). Such an offset might simply reflect the fact that incident solar radiation at the top of the atmosphere decreases poleward, which reduces the surface shortwave radiative impact of a given change in cloud fraction (for the same cloud optical depth) compared to lower latitudes (Zelinka et al., 2012). Regardless of the physics explaining the offset, it is nonetheless clear that a positive cloud feedback did not amplify or increase the persistence of this warm water Blob.

Instead, Figures 4c and 4d illustrate that a combination of anomalous wind-driven turbulent heat flux and total oceanic heat flux provided the principal contribution to the anomalous energy budget of the ocean mixed layer during this January-to-December 2013 warming event. Spatially averaged turbulent flux, total oceanic flux, and horizontal advection anomalies of 12.7 ± 4.7, 10 ± 8.2, and 9.7 ± 5.1 W/m^2 within the region of maximum warming in 2013 indicate that weaker surface westerlies were responsible for both reduced surface turbulent heat flux loss and Ekman transport from cooler northern waters (Table S1 and Figures S5, S8, and S11). Spatially averaged values computed using turbulent flux data from ERA-Interim instead suggest that almost all of the warming was driven by anomalous sensible and latent heat fluxes and that the total oceanic flux was not discernibly different than average (Table S1). By explicitly quantifying which surface fluxes contributed to the warming, this analysis expands upon previous findings that identified reduced surface heat loss and horizontal advection as key to the occurrence of the Blob (Bond et al., 2015; Liang et al., 2017).

6. Conclusions

An analysis of the energy budget of the ocean mixed layer reveals that distinct mechanisms were responsible for the record-breaking warm subtropical anomalies, off Baja California, and warm midlatitude anomalies,

near the Gulf of Alaska, of the 2013–2015 NE Pacific marine heatwave. Off Baja California, a very large decrease in low cloud coverage and a very large increase in the amount of solar radiation reaching the ocean surface over a nearly two-year period explain why SST in the region warmed to such a high magnitude. Over the Gulf of Alaska region, a very large decrease in ocean-to-atmosphere turbulent heat flux combined with anomalous heating of the mixed layer due to ocean processes over a one-year period explains the emergence of the intense warm SST Blob anomaly. Offsetting components of surface shortwave and longwave CRE despite a decrease in low cloud coverage over the Blob implies that the reduction in cloudiness did not act as a positive feedback on SST in that midlatitude region of the NE Pacific marine heatwave.

Contrastingly, our results provide observational evidence strongly suggesting that low clouds intensely amplified surface temperature anomalies in the subtropical region of the NE Pacific marine heatwave. This amplification contributed to a transition to the warm phase of Pacific decadal variability. These observation-based findings demonstrate that a positive feedback between low clouds and ocean surface temperature can be an order one process in regional climate fluctuations.

Acknowledgments

This study was funded by NOAA's Climate Program Office, Climate Variability and Predictability Program award NA14OAR4310278. G. C. was supported by a CloudSat-CALIPSO RTOP at the Goddard Institute for Space Studies. M. D.'s and D. W.'s contributions to this study were carried out on behalf of the Jet Propulsion Laboratory, California Institute of Technology, under a contract with the National Aeronautics and Space Administration. Joel Norris kindly provided the monthly averaged ISCCP data. The authors acknowledge helpful discussions with Jin-Yi Yu and also thank the reviewers for their effort in reading and thoughtfully commenting on the submitted manuscript. Data used in the study are available for download from https://www.esrl.noaa.gov/psd/data/gridded/ (NOAA OI SST, NOAA ERSTv4, and GODAS), http://research.jisao.washington.edu/pdo/PDO.latest.txt (PDO index), https://ceres.larc.nasa.gov/ (CERES and MODIS), http://oaflux.whoi.edu (OAFlux), http://apps.ecmwf.int/datasets/ (ERA-Interim), http://climserv.ipsl.polytechnique.fr/cfmip-obs/Calipso_goccp.html (CALIPSO), https://isccp.giss.nasa.gov/ ("original" ISCCP), and https://doi.org/10.5065/D62J68XR ("corrected" ISCCP).

References

Amaya, D. J., Bond, N. E., Miller, A. J., & DeFlorio, M. J. (2016). The evolution and known atmospheric forcing mechanisms behind the 2013-2015 North Pacific warm anomalies. *US Clivar Variations*, *14*, 1–6.

Behringer, D. W. (2007). The Global Ocean Data Assimilation System (GODAS) at NCEP, paper 3.3 presented at 11th Symp. on Integrated Observing and Assimilation Systems for Atmosphere, Oceans, and Land Surface, Am. Meteorol. Soc., San Antonio, Tex., Preprints. Retrieved from http://ams.confex.com/ams/87ANNUAL/techprogram/paper_119541.htm

Behringer, D. W., & Xue, Y. (2004). Evaluation of the Global Ocean Data Assimilation System at NCEP: The Pacific Ocean, paper 2.3 presented at Eighth Symp. on Integrated Observing and Assimilation Systems for Atmosphere, Oceans, and Land Surface, Am. Meteorol. Soc., Seattle, Wash., Preprints. Retrieved from http://ams.confex.com/ams/84Annual/techprogram/paper_70720.htm

Bellomo, K., Clement, A., Mauritsen, T., Rädel, G., & Stevens, B. (2014). Simulating the role of subtropical stratocumulus clouds in driving Pacific climate variability. *Journal of Climate*, *27*(13), 5119–5131. https://doi.org/10.1175/JCLI-D-13-00548.1

Bellomo, K., Clement, A., Mauritsen, T., Rädel, G., & Stevens, B. (2015). The influence of cloud feedbacks on equatorial Atlantic variability. *Journal of Climate*, *28*(7), 2725–2744. https://doi.org/10.1175/JCLI-D-14-00495.1

Bellomo, K., Clement, A. C., Murphy, L. N., Polvani, L., & Cane, M. A. (2016). New observational evidence for a positive cloud feedback that amplifies the Atlantic multidecadal oscillation. *Geophysical Research Letters*, *43*, 9852–9859. https://doi.org/10.1002/2016GL069961

Bond, N. A., Cronin, M. F., Freeland, H., & Mantua, N. (2015). Causes and impacts of the 2014 warm anomaly in the NE Pacific. *Geophysical Research Letters*, *42*, 3414–3420. https://doi.org/10.1002/2015GL063306

Bretherton, C. S., Blossey, P. N., & Jones, C. R. (2013). Mechanisms of marine low cloud sensitivity to idealized climate perturbations: A single-LES exploration extending the CGILS cases. *Journal of Advances in Modeling Earth Systems*, *5*(2), 316–337. https://doi.org/10.1002/jame.20019

Brown, P. T., Lozier, M. S., Zhang, R., & Li, W. (2016). The necessity of cloud feedback for a basin-scale Atlantic Multidecadal Oscillation. *Geophysical Research Letters*, *43*, 3955–3963. https://doi.org/10.1002/2016GL068303

Burgman, R. J., Kirtman, B. P., Clement, A. C., & Vazquez, H. (2017). Model evidence for low-level cloud feedback driving persistent changes in atmospheric circulation and regional hydroclimate. *Geophysical Research Letters*, *44*, 428–437. https://doi.org/10.1002/2016GL071978

Cavole, L. M., Demko, A. M., Diner, R. E., Giddings, A., Koester, I., Pagniello, C. M. L. S., et al. (2016). Biological impacts of the 2013–2015 warm-water anomaly in the Northeast Pacific: Winners, losers, and the future. *Oceanography*, *29*, 273–285.

Cesana, G., Chepfer, H., Winker, D., Getzewich, B., Cai, X., Jourdan, O., et al. (2016). Using in-situ airborne measurements to evaluate three cloud phase products derived from CALIPSO. *Journal of Geophysical Research: Atmospheres*, *121*, 5788–5808. https://doi.org/10.1002/2015JD024334

Chepfer, H., Bony, S., Winker, D., Cesana, G., Dufresne, J. L., Minnis, P., et al. (2010). The GCM-oriented CALIPSO cloud product (CALIPSO-GOCCP). *Journal of Geophysical Research*, *115*, D00H16. https://doi.org/10.1029/2009JD012251

Dee, D. P., Uppala, S., Simmons, A., Berrisford, P., Poli, P., Kobayashi, S., et al. (2011). The ERA-Interim reanalysis: Configuration and performance of the data assimilation system. *Quarterly Journal of the Royal Meteorological Society*, *137*(656), 553–597. https://doi.org/10.1002/qj.828

Di Lorenzo, E., & Mantua, N. (2016). Multi-year persistence of the 2014/15 North Pacific marine heatwave. *Nature Climate Change*, *6*(11), 1042–1047. https://doi.org/10.1038/nclimate3082

Feng, J., Wu, Z., & Zou, X. (2014). Sea surface temperature anomalies off Baja California: A possible precursor of ENSO. *Journal of the Atmospheric Sciences*, *71*(5), 1529–1537. https://doi.org/10.1175/JAS-D-13-0397.1

Garay, M. J., de Szoeke, S. P., & Moroney, C. M. (2008). Comparison of marine stratocumulus cloud top heights in the southeastern Pacific retrieved from satellites with coincident ship-based observations. *Journal of Geophysical Research*, *113*, D18204. https://doi.org/10.1029/2008JD009975

Gentemann, C. L., Fewings, M. R., & García-Reyes, M. (2017). Satellite sea surface temperatures along the West Coast of the United States during the 2014–2016 northeast Pacific marine heat wave. *Geophysical Research Letters*, *44*, 312–319. https://doi.org/10.1002/2016GL071039

Hartmann, D. L., Ockert-Bell, M. E., & Michelsen, M. L. (1992). The effect of cloud type on Earth's energy balance: Global analysis. *Journal of Climate*, *5*(11), 1281–1304. https://doi.org/10.1175/1520-0442(1992)005<1281:TEOCTO>2.0.CO;2

Huang, B., Banzon, V. F., Freeman, E., Lawrimore, J., Liu, W., Peterson, T. C., et al. (2014). Extended Reconstructed Sea Surface Temperature version 4 (ERSST.v4): Part I. Upgrades and intercomparisons. *Journal of Climate*, *28*, 911–930.

Jacox, M. G., Alexander, M. A., Mantua, N. J., Scott, J. D., Hervieux, G., Webb, R. S., & Werner, F. E. (2018). Forcing of multiyear extreme ocean temperatures that impacted California Current living marine resources in 2016 [in "Explaining extreme events of 2016 from a climate perspective"]. *Bulletin of the American Meteorological Society*, *98*, S27–S33.

Kato, S., & Loeb, N. G. (2013). Surface irradiances consistent with CERES-derived top-of-atmosphere shortwave and longwave irradiances. *Journal of Climate*, *26*(9), 2719–2740. https://doi.org/10.1175/JCLI-D-12-00436.1

Klein, S. A., Hall, A., Norris, J. R., & Pincus, R. (2017). Low-cloud feedbacks from cloud-controlling factors: A review. *Surveys in Geophysics*, 1–23.

Klein, S. A., & Hartmann, D. L. (1993). The seasonal cycle of low stratiform clouds. *Journal of Climate*, *6*(8), 1587–1606. https://doi.org/10.1175/1520-0442(1993)006<1587:TSCOLS>2.0.CO;2

Large, W. G., McWilliams, J. C., & Doney, S. C. (1994). Oceanic vertical mixing: A review and a model with a nonlocal boundary layer parameterization. *Reviews of Geophysics*, *32*, 363–403. https://doi.org/10.1029/94RG01872

Liang, Y. -C., Yu, J. -Y., & Saltzman, E. S. (2017). Linking the tropical northern hemisphere pattern to the Pacific warm blob and Atlantic cold blob. *Journal of Climate*, *30*(22), 9041–9057. https://doi.org/10.1175/JCLI-D-17-0149.1

Minnis, P., Sun-Mack, S., Young, D. F., Heck, P. W., Garber, D. P., Chen, Y., et al. (2011). CERES edition-2 cloud property retrievals using TRMM VIRS and Terra and Aqua MODIS data—Part I: Algorithms. *IEEE Transactions on Geoscience and Remote Sensing*, *49*(11), 4374–4400. https://doi.org/10.1109/TGRS.2011.2144601

Myers, T. A., Mechoso, C. R., & DeFlorio, M. J. (2017). Importance of positive cloud feedback for tropical Atlantic interhemispheric climate variability. *Climate Dynamics*. https://doi.org/10.1007/s00382-017-3978-1

Myers, T. A., Mechoso, C. R., & DeFlorio, M. J. (2018). Coupling between marine boundary layer clouds and summer-to-summer sea surface temperature variability over the North Atlantic and Pacific. *Climate Dynamics*, *50*(3-4), 955–969. https://doi.org/10.1007/s00382-017-3651-8

Norris, J. R., & Evan, A. T. (2015). Empirical removal of artifacts from the ISCCP and PATMOS-x satellite cloud records. *Journal of Atmospheric and Oceanic Technology*, *32*(4), 691–702. https://doi.org/10.1175/JTECH-D-14-00058.1

Paek, H., Yu, J. -Y., & Qian, C. (2017). Why were the 2015/2016 and 1997/1998 extreme El Niños different? *Geophysical Research Letters*, *44*, 1848–1856.

Park, S., Deser, C., & Alexander, M. A. (2005). Estimation of the surface heat flux response to sea surface temperature anomalies over the global oceans. *Journal of Climate*, *18*(21), 4582–4599. https://doi.org/10.1175/JCLI3521.1

Reynolds, R. W., Rayner, N. A., Smith, T. M., Stokes, D. C., & Wang, W. (2002). An improved in situ and satellite SST analysis for climate. *Journal of Climate*, *15*(13), 1609–1625. https://doi.org/10.1175/1520-0442(2002)015<1609:AIISAS>2.0.CO;2

Rieck, M., Nuijens, L., & Stevens, B. (2012). Marine boundary layer cloud feedbacks in a constant relative humidity atmosphere. *Journal of the Atmospheric Sciences*, *69*(8), 2538–2550. https://doi.org/10.1175/JAS-D-11-0203.1

Robinson, C. J. (2016). Evolution of the 2014–2015 sea surface temperature warming in the central west coast of Baja California, Mexico, recorded by remote sensing. *Geophysical Research Letters*, *43*(13), 7066–7071. https://doi.org/10.1002/2016GL069356

Rossow, W. B., & Schiffer, R. A. (1999). Advances in understanding clouds from ISCCP. *Bulletin of the American Meteorological Society*, *80*(11), 2261–2287. https://doi.org/10.1175/1520-0477(1999)080<2261:AIUCFI>2.0.CO;2

Seager, R., Hoerling, M., Schubert, S., Wang, H., Lyon, B., Kumar, A., et al. (2015). Causes of the 2011–14 California drought. *Journal of Climate*, *28*(18), 6997–7024. https://doi.org/10.1175/JCLI-D-14-00860.1

Su, J., Zhang, R., & Wang, H. (2017). Consecutive record-breaking high temperatures marked the handover from hiatus to accelerated warming. *Scientific Reports*, *7*.

Swain, D. L., Tsiang, M., Haugen, M., Singh, D., Charland, A., Rajaratnam, B., & Diffenbaugh, N. S. (2014). The extraordinary California drought of 2013/14: Character, context and the role of climate change. *Bulletin of the American Meteorological Society*, *95*.

Tseng, Y. H., Ding, R., & Huang, X. M. (2017). The warm Blob in the northeast Pacific—The bridge leading to the 2015/16 El Niño. *Environmental Research Letters*, *12*(5), 054019. https://doi.org/10.1088/1748-9326/aa67c3

van der Dussen, J. J., de Roode, S. R., Gesso, S. D., & Siebesma, A. P. (2015). An LES model study of the influence of the free troposphere on the stratocumulus response to a climate perturbation. *Journal of Advances in Modeling Earth Systems*, *7*(2), 670–691. https://doi.org/10.1002/2014MS000380

Yu, J. -Y., Liu, W. T., & Mechoso, C. R. (2000). An SST anomaly dipole in the northern subtropical Pacific and its relationships with ENSO. *Geophysical Research Letters*, *27*, 1931–1934. https://doi.org/10.1029/1999GL011340

Yu, L., Jin, X., & Weller, R. A. (2008). Multidecade global flux datasets from the objectively analyzed air-sea fluxes (OAFlux) project: Latent and sensible heat fluxes, ocean evaporation, and related surface meteorological variables, Tech. Rep. OA-2008-01, Woods Hole Oceanogr. Inst., Woods Hole, Mass.

Zaba, K. D., & Rudnick, D. L. (2016). The 2014–2015 warming anomaly in the Southern California Current System observed by underwater gliders. *Geophysical Research Letters*, *43*, 1241–1248. https://doi.org/10.1002/2015GL067550

Zelinka, M. D., Klein, S. A., & Hartmann, D. L. (2012). Computing and partitioning cloud feedbacks using cloud property histograms. Part I: Cloud radiative kernels. *Journal of Climate*, *25*(11), 3715–3735. https://doi.org/10.1175/JCLI-D-11-00248.1